Chinese Chemical Letters 36 (2025) 110235

Contents lists available at ScienceDirect

Chinese Chemical Letters

journal homepage: www.elsevier.com/locate/cclet

Regulating local electron transfer environment of covalent triazine frameworks through F, N co-modification towards optimized oxygen reduction reaction

Quanyou Guo[1], Yue Yang[1], Tingting Hu, Hongqi Chu*, Lijun Liao, Xuepeng Wang, Zhenzi Li, Liping Guo*, Wei Zhou*

Shandong Provincial Key Laboratory of Molecular Engineering, School of Chemistry and Chemical Engineering, Qilu University of Technology (Shandong Academy of Sciences), Ji'nan 250353, China

ARTICLE INFO

Article history:
Received 7 May 2024
Revised 4 July 2024
Accepted 10 July 2024
Available online 11 July 2024

Keywords:
Covalent triazine frameworks
Conductivity
Co-modification
Electrocatalysis
Oxygen reduction reaction

ABSTRACT

The high conductivity of electrocatalyst can eliminate the Schottky energy barrier at the interface of heterogeneous phases during an electrocatalytic reaction and accelerate the rapid electron transfer to the catalytic active center. Therefore, the electronic conductivity is a vital parameter for oxygen reduction reaction (ORR). Covalent triazine frameworks (CTFs) have shown great potential application as electrocatalysts in ORR with a merit of the diverse building blocks. However, the intrinsic low conductivity and high impedance of CTFs could be significant setbacks in electrocatalytic application. Herein, CTFs were constructed by introducing F and N co-modification for efficient $2e^-$ ORR. Compared with the pristine CTF, the co-presence of F, N could increase the conductivity obviously by 1000-fold. As a result, F-N-CTF exhibits enhanced catalytic performance of H_2O_2 generation and selectivity towards reaction pathways. This work reveals the importance of conductivity optimization for CTFs and provides guidance for designing high conductivity non-metallic organic semiconductor catalysts for $2e^-$ ORR.

As the global energy crisis and environmental problems continue to worsen, there is a growing need for clean energy conversion devices like fuel cells [1]. The oxygen reduction reaction (ORR), which is the cathodic process in fuel cells, plays a pivotal role in augmenting their operational efficacy [2]. Nonetheless, relative to the anodic oxidation reaction, the ORR exhibits considerably diminished reaction kinetics, thereby imposing severe constraints on the advancement of fuel cell performance [3,4]. Currently, commercial platinum-based catalysts are employed to facilitate the sluggish kinetics of the ORR [5,6]. However, the drawbacks associated with such catalysts, including limited reserves and exorbitant costs, impede the widespread application of fuel cells [7]. Consequently, there is an imperative need to develop affordable and efficient catalysts for ORR [8]. In recent years, heteroatom doping has emerged as a proven method for preparing ORR catalysts that are both efficient and cost-effective [9,10]. Essential criteria for these materials encompass a high specific surface area and a robust porous structure, which facilitate the exposure of numerous electrocatalytic active sites and expedite the transport of relevant species [11–13].

Currently, catalysts used for electrocatalytic ORR can be roughly divided into four categories: transition metal complexes [14], inorganic semiconductors [15,16], metal-organic frameworks (MOFs) [17,18], and covalent organic frameworks (COFs) [19–21]. Among them, covalent organic frameworks, especially covalent triazine frameworks (CTFs), have received considerable attention in recent years [22–24]. This is mainly due to the fact that CTFs are porous organic polymers with ordered structures, large surface areas, high chemical and thermal stability, structural diversity, and precise atomic positions, which determine their wide range of applications [25,26]. However, they do suffer from issues such as poor conductivity. To further improve the electrocatalytic ORR performance of CTF materials, it is necessary to establish a structure-performance relationship and adopt corresponding strategies to overcome the poor conductivity issue [27,28]. Therefore, developing low-cost ORR catalysts is crucial for practical applications of electrocatalytic ORR [29,30].

Non-metal doping is an effective strategy to improve the electronic transfer efficiency of materials [31–34]. Halogens are

* Corresponding authors.
E-mail addresses: hqchu@qlu.edu.cn (H. Chu), guoliping@qlu.edu.cn (L. Guo), zwchem@hotmail.com (W. Zhou).
[1] These authors contributed equally to this work.

https://doi.org/10.1016/j.cclet.2024.110235
1001-8417/

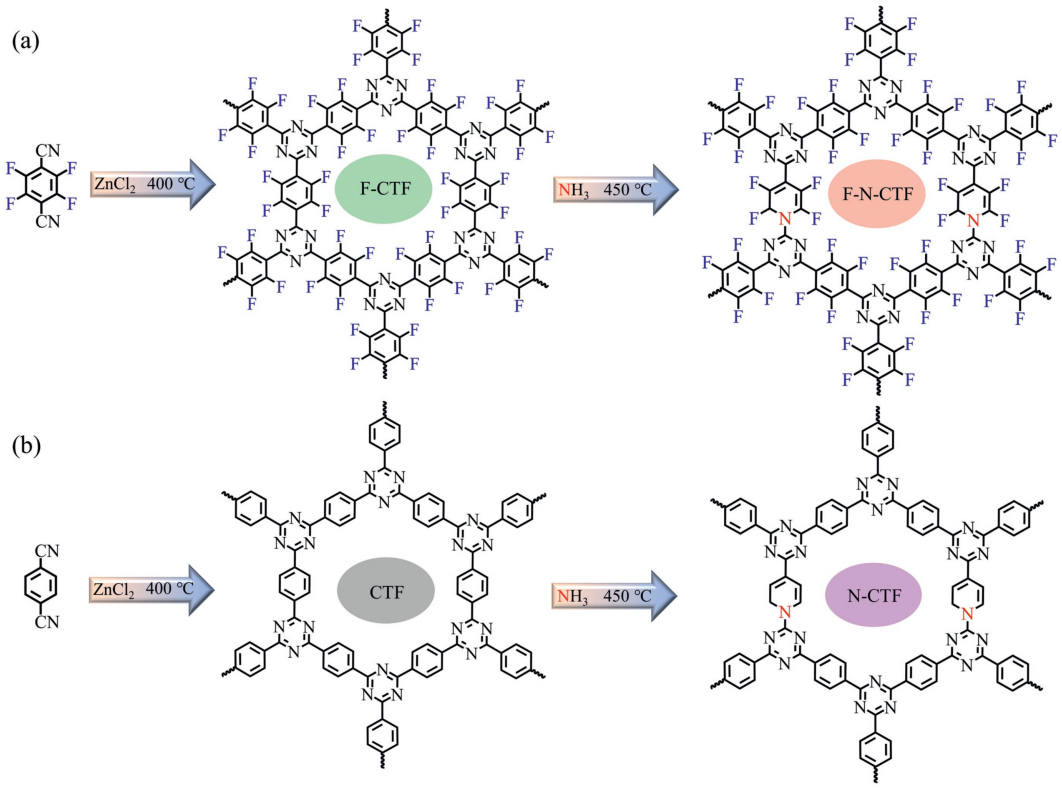

Fig. 1. Schematic illustration for the fabrication of (a) F-CTF and F-N-CTF, and (b) CTF and N-CTF.

located on the left side of the periodic table and have strong electronegativity, making them electron acceptor sites [35–37]. Introducing halogens can significantly affect the electronic structure of the matrix, thereby influencing the final charge transfer performance. Fluorine-containing CTFs are rare in their composition, but they offer interesting properties associated with this highly electronegative atom [38]. In fact, fluorinated materials often exhibit unique properties, such as inverted charge distribution in benzene rings. F atoms have small atomic sizes and high electronegativity. It has been reported that F atoms are more prone to replace nitrogen (N) atoms and form C-F bonds in g-C_3N_4 [39]. Nitrogen doping is also a strategy to enhance the electronic conductivity of materials [40,41]. Because N and C have similar atomic radii, lattice mismatch can be prevented. In addition, N has one more electron than C, which is advantageous for reactions requiring electron participation, such as ORR [42,43]. Therefore, N as a dopant element can effectively improve the performance of sp^2 carbon as an ORR electrocatalyst. The improved ORR performance of nitrogen-doped graphene (G) is attributed to the charge transfer facilitation induced by N dopants in the graphitic framework and the relatively lower overpotential for oxygen adsorption, as proposed by the Dai group [44]. Increasing the nitrogen content by treating the material with ammonia can increase the number of active sites, thereby improving the electrocatalytic ORR performance.

Based on the above, we synthesized a F and N co-modificated covalent triazine framework material. By fully utilizing the high reactivity of triazine groups, the synthesis of fluorine-doped covalent triazine framework materials is modified, and further nitrogen doping is achieved through ammonia treatment to increase the nitrogen content (Fig. 1a). As a comparison, the CTF without F was used in this work (Fig. 1b). This method helps to improve the electrocatalytic ORR performance obviously.

Transmission electron microscopy (TEM) images show that the CTF, F-CTF, N-CTF, and F-N-CTF have similar sheet structure in Figs. 2a–d [45]. Scanning electron microscope (SEM) show no obvious appearance difference before and after calcination (Figs. S1a-d in Supporting information). As shown in Figs. 2e–h, the elemental mapping image shows that C, N, O, F were evenly distributed in the catalysts, confirming the doping of N and F in F-N-CTF samples [46]. Fig. 2i portrays the infrared spectra of the samples, where distinct peaks of C-N and C=N can be discerned at 1351 cm^{-1} and 1520 cm^{-1}, respectively, signifying the formation of the triazine ring structure. Furthermore, for F-CTF and F-N-CTF, peaks corresponding to the C-F bond become visible around 1104 cm^{-1} indicate the successful introduction of fluorine (F) [47]. Both of these CTFs show high thermal stability (Fig. S2 in Supporting information). Disordered structure and low crystallinity can be observed in Fig. S3 (Supporting information). Due to the lower temperature than that of systhesis process, the ammonia calcination impact little on the porous structure of CTFs (Fig. 2j and Fig. S4 in Supporting information). According to the N_2 sorption performance, the specific surface areas of these CTFs are close to each other. Compare to other CTF, F-N-CTF expresses a slight bigger Brunauer-Emmett-Teller (BET) surface area (618 m^2/g), which could support more active sites for catalysis. The elemental composition of the sample is delineated in Table S1 (Supporting information). After ammonia calcination, F-N-CTF and N-CTF have higher content of N than F-CTF and CTF, respectively. These results indicate the successful introduction of F and N.

To explore the N doping position in CTF skeletons, X-ray photoelectron spectroscopy (XPS) was employed in this work (Fig. 3). F-CTF and F-N-CTF have obvious characteristic peaks of F and N (Fig. 3a), indicating the successful introduction of F and N elements into the catalyst. After calcination in the presence of ammonia, the proportion of N-C in N-CTF and N-F-CTF significantly increased (Fig. 3b). Compared with the high-resolution XPS spectra of C 1s (Fig. 3c), the binding energy of C in triazine ring in N-CTF (286.6 eV) and in F-N-CTF (286.4 eV) increased obviously

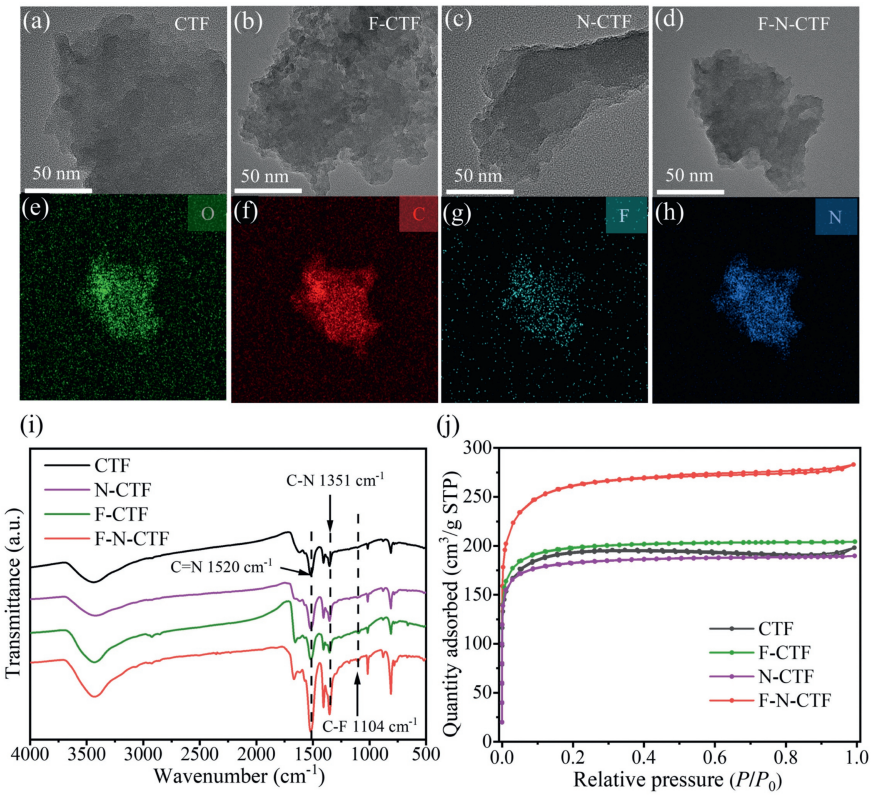

Fig. 2. Transmission electron microscopy (TEM) images of CTF (a), F-CTF (b), N-CTF (c), and F-N-CTF (d). (e–h) EDS-mapping images of F-N-CTF. (i) FTIR spectra of CTFs. (j) N_2 adsorption−desorption isotherms of CTF, F-CTF, N-CTF, and F-N-CTF.

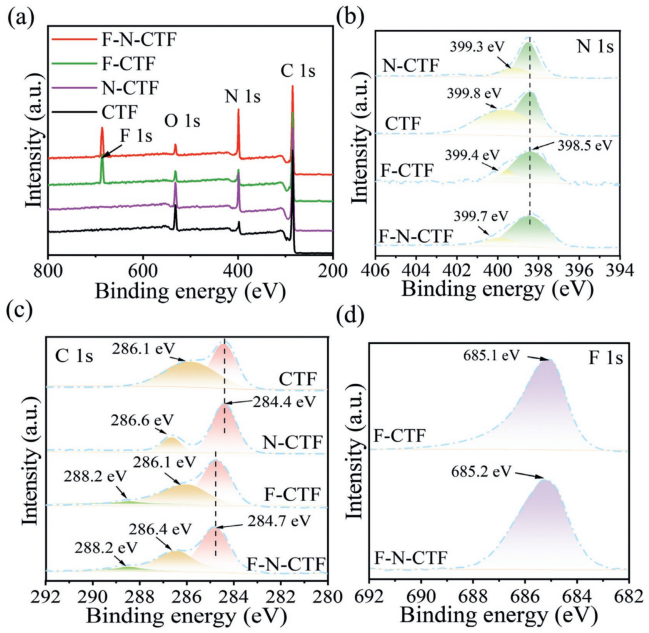

Fig. 3. (a) The XPS survey spectra of CTF, F-CTF, N-CTF, F-N-CTF. XPS of F 1s (b), N 1s (c), C 1s (d) for CTF, F-CTF, N-CTF, and F-N-CTF.

after calcination with ammonia. The increased binding energy of C in triazine illustrates the presence of N doping in the benzene ring neighboring the triazine ring, in which N would more easily accept electrons than C. Furthermore, there is no newly formed bond (*e.g.*, N-F) according to the high-resolution XPS spectra of F 1s (Fig. 3d), thereby proving that the doped N substitutes the carbon in the benzene ring connected with the triazine ring.

In addition, the electrocatalytic activity of the four specimens in the ORR within a 0.1 mol/L KOH solution was examined at ambient temperature, a rotational speed of 1600 revolutions per minute (rpm), and a scan rate of 10 mV/s [48]. The polarization curves (Figs. 4a and b, and Fig. S5 in Supporting information) provide a clear representation of the relative catalytic activities of the three samples in promoting ORR, with the following order observed: CTF < F-CTF < N-CTF < F-N-CTF. This finding suggests that incorporating fluorine and nitrogen during the synthesis process notably enhances the catalytic activity. Specifically, F-N-CTF exhibits values of initial potential (E_{onset}), half-wave potential ($E_{1/2}$), and the limiting current density (J_L) equal to 0.73 V, 0.51 V, and 0.51 mA/cm^2, respectively. These values are considerably higher than the corresponding parameters for CTF, N-CTF, and F-CTF [49]. Moreover, the Tafel slope for F-N-CTF was measured at 66.5 mV/dec, which is lower than CTF, N-CTF, and F-CTF (Fig. 4c) [50,51]. This can illustrate that after N and F modification, the material exhibited excellent reaction kinetics [52,53]. In Fig. 4d the average electrons number (n) of the overall oxygen reduction reaction of CTF, F-CTF, N-CTF, and F-N-CTF was determined to be 0.64, 0.86, 0.95, and 1.51, respectively, by the slope of the linear regression. The data indicate that the presence of F-C and C=N bonds enabled F-N-CTF to achieve ORR through the 2e$^-$ pathway and exhibited high activity and selectivity [54].

Moreover, the performance for H_2O_2 generation of F-N-CTF was evaluated in a three-electrode system equipped with a H-type electrolytic cell different potential (0.1, 0.2, 0.3, 0.4 and 0.5 V *vs.* RHE) (Fig. 4e and Fig. S6 in Supporting information). As shown in Fig. 4e, the rate and Faraday efficiency of H_2O_2 generation were measured by time current curve test about 1 h. The result show that the optimized H_2O_2 generation rate at 0.1 V *vs.* RHE is up to 26 mg L^{-1} h^{-1}

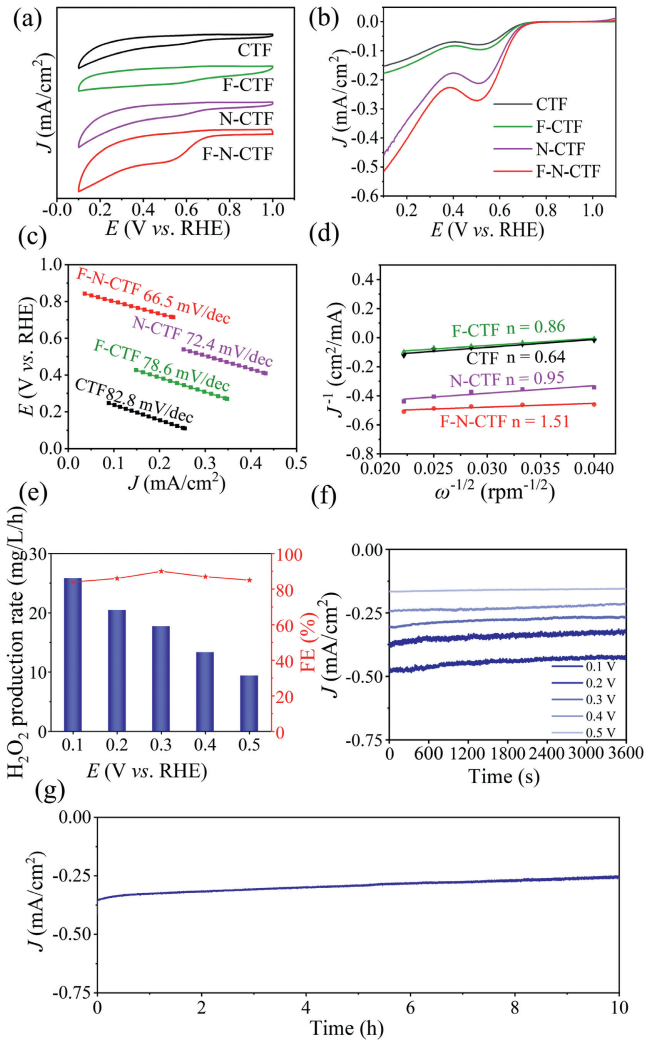

Fig. 4. (a) CVs of CTF, F-CTF, N-CTF, F-N-CTF. (b) LSVs of CTF, F-CTF, N-CTF, F-N-CTF. (c) Tafel slope curve diagram. (d) Number of transfer electrons for CTF, F-CTF, N-CTF, and F-N-CTF. (e) H_2O_2 production rate and Faraday efficiency at different potentials. (f) Time-current density of F-N-CTF at different potentials curves. (g) The time-current density curve for 10 h.

and the highest Faraday efficiency can reach up to 94% among these testing potentials. This performance is comparable than other metal-free electrocatalyst (Table S2 in Supporting information). The turnover frequency (TOF) and mass activity (Ma) were evaluated (Fig. S7 in Supporting information) and the value of F-N-CTF is 0.94 s^{-1} and Ma is 0.39 A/mg_N. In addition, the oxygen reduction selectivity of F-N-CTF to H_2O_2 was measured using a rotating ring disk electrode in a 0.1 mol/L KOH electrolyte. According to the calculation of the test results, the selectivity of F-N-CTF for generating hydrogen peroxide through oxygen reduction is 69% (Fig. S8 in Supporting information). Stability is also an important indicator to evaluate the performance of catalysts. The time-current density curves at various five potentials were recorded (Fig. 4f). The results show that the reduction current is gradually increased by decreasing applied potential. Both of these current densities exhibit high stability at various five potentials. In order to further evaluate the durability and stability of F-N-CTF under operating conditions, a long-term time current curve test of the F-N-CTF was performed for 10 h using an H-type electrolytic cell. Figs. 4f and g show that F-N-CTF exhibits high stability at different current density within 1 h, and this target CTF also keep long-term stability with retention approximately 90% after 10 h in 0.1 mol/L KOH electrolyte. After the stability testing of 10 h, the morphology and structure of F-N-CTF are well retained (Figs. S9 and S10 in Supporting information). The high stability of CTF ensures the stability of catalytic performance.

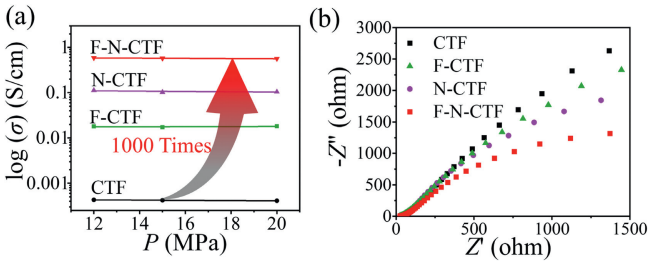

Fig. 5. (a) Conductivity test of CTF, F-CTF, N-CTF, F-N-CTF. (b) EIS spectra of CTF, F-CTF, N-CTF, and F-N-CTF.

To explor the enhanced performance of 2e⁻ ORR of F-N-CTF, the electronic structure of CTFs was firstly evaluated by electron paramagnetic resonance (EPR) characterization. According to the EPR results in Fig. S11 (Supporting information), the enhanced response is observed with the F presence in CTF. Besides, the N introduction would further increase the EPR signal. The highest EPR intensity of F-N-CTF illustrates the more delocalized structure, which is much positive to charge transfer [55]. Moreover, the electrnoic conductivity was measured. The results show that the introduction of both fluorine and nitrogen would increase conductivity obviously. The F-N-CTF exhibit remarkable highest electrical conductivity up to 8.3 S/cm, which is about 1000-fold than that of prisitne CTF (Fig. 5a). The high conductivity is conducive to the electron transfer during the catalytic process. Moreover, the electrochemical impedance spectroscopies (EIS) were also tested of these CTFs. The smaller the line radius of EIS is, the little the charge transport resistance it will have. As shown in Fig. 5b, the N-F-CTF demonstrated the smallest charge transfer resistance, which may be due to the introduction of F and N to regulate local electron transfer environment of the F-N-CTF, thereby enhancing the ORR performance.

In conclusion, the F was firstly introduced with the *in-situ* method and then the N was further doped into CTF skeletons to form C=N bonds under ammonia treatment. The F-C and C=N bonds enabled the targeting F-N-CTF high electronic conductivity by approximately 1000-fold and much smaller charge transport resistance. Therefore, F-N-CTF achieve ORR through the 2e⁻ pathway with high activity and selectivity. Due to the synergistic effect of F and N, the local electron transfer environment is optimized. Therefore, CTF can generate fast electron and ion transport pathways, significantly improving electrocatalytic activity. This new F and N modification strategy of CTFs opens up a new avenue for manufacturing high conductivity non-metallic CTFs organic catalysts for 2e⁻ ORR.

Declaration of competing interest

The authors declare that they have no known competing financial interests or personal relationships that could have appeared to influence the work reported in this paper.

CRediT authorship contribution statement

Quanyou Guo: Formal analysis, Data curation. **Yue Yang:** Investigation, Formal analysis. **Tingting Hu:** Software, Methodology. **Hongqi Chu:** Writing – original draft, Supervision. **Lijun Liao:** Validation, Investigation. **Xuepeng Wang:** Visualization, Investigation. **Zhenzi Li:** Visualization. **Liping Guo:** Writing – review & edit-

ing, Funding acquisition, Conceptualization. **Wei Zhou:** Supervision, Funding acquisition, Conceptualization.

Acknowledgments

We give thanks for the financial support by the National Natural Science Foundation of China (Nos. 22205124, 52172206), Natural Science Foundation of Shandong province (Nos. ZR2021QB070, ZR2023QB110), Basic Research Projects for the Pilot Project of Integrating Science and Education and Industry of Qilu University of Technology (Shandong Academy of Sciences) (Nos. 2023PY024, 2023PX108), Special Fund for Taishan Scholars Project, and the Development Plan of Youth Innovation Team in Colleges and Universities of Shandong Province.

Supplementary materials

Supplementary material associated with this article can be found, in the online version, at doi:10.1016/j.cclet.2024.110235.

References

[1] J. Xu, P. Wang, Z. Bai, et al., Nat. Rev. Mater. 9 (2024) 722–737.
[2] M. Martínez-Fernández, E. Martínez-Periñán, A. de la Peña Ruigómez, et al., Angew. Chem. Int. Ed. 62 (2023) e202313940.
[3] Z. Li, H. Cheng, Y. Lu, et al., Adv. Energy Mater. 13 (2023) 2203963.
[4] X. Cui, M. Wu, X. Liu, et al., Chem. Soc. Rev. 53 (2024) 1447–1494.
[5] Z.Y. Mei, G. Zhao, C. Xia, et al., Angew. Chem. Int. Ed. 62 (2023) e202303871.
[6] X. Zhang, Z. Wang, A.M. Lawan, et al., InfoMat 5 (2023) e12406.
[7] X. Yan, B. Wang, J. Ren, et al., Angew. Chem. Int. Ed. 61 (2022) e202209583.
[8] X. Li, S. Yang, M. Liu, et al., Small Struct. 4 (2023) 2200320.
[9] Z. You, B. Wang, Z. Zhao, et al., Adv. Mater. 35 (2023) 2209129.
[10] S.D. Bhoyate, J. Kim, F.M. de Souza, et al., Coord. Chem. Rev. 474 (2023) 214854.
[11] S. Mondal, B. Mohanty, M. Nurhuda, et al., ACS Catal. 10 (2020) 5623–5630.
[12] J. Zhen, J. Shen, T. Sun, et al., CCS Chem. 6 (2024) 932–940.
[13] Z. Gu, Z. Shan, Y. Wang, et al., Chin. Chem. Lett. 35 (2024) 108356.
[14] J. Cai, H. Zhang, L. Zhang, et al., Adv. Mater. 35 (2023) 2303488.
[15] G. Lv, Y. Wu, Y. Wang, et al., Nano Energy 76 (2020) 105055.
[16] J. Ran, L. Wang, M. Si, et al., Small 19 (2022) 2206367.
[17] Z. Liang, H. Guo, G. Zhou, et al., Angew. Chem. Int. Ed. 60 (2021) 8472–8476.
[18] Q.H. Nguyen, V.D.C. Tinh, S. Oh, et al., Chem. Eng. J. 481 (2024) 148508.
[19] X. Li, Y. Fu, Q. An, et al., Appl. Catal. B 344 (2024) 123611.
[20] L. Xiao, L. Qi, J. Sun, et al., Nano Energy 120 (2024) 109155.
[21] N. Arora, C. Flores, M.C. Senarathna, et al., CCS Chem. 6 (2024) 57–68.
[22] S. Li, M.F. Wu, T. Guo, et al., Appl. Catal. B 272 (2020) 118989.
[23] K. Cui, X. Tang, X. Xu, et al., Angew. Chem. Int. Ed. 63 (2024) e202317664.
[24] Y. Zheng, S. Chen, K.A.I. Zhang, et al., ACS Appl. Mater. Interfaces 13 (2021) 13328–13337.
[25] W. Huang, N. Huber, S. Jiang, et al., Angew. Chem. Int. Ed. 59 (2020) 18368–18373.
[26] J. Wang, X. Lian, X. Cao, et al., Chin. Chem. Lett. 35 (2024) 109180.
[27] L. Guan, Z. Guo, Q. Zhou, et al., Nat. Commun. 14 (2023) 8114.
[28] Z. Zheng, X. Hong, D. Wu, et al., Adv. Compos. Hybrid Mater. 6 (2023) 90.
[29] S. Zhang, J. Zheng, J. Lin, et al., Nano Res. 16 (2023) 6120–6127.
[30] X. Yang, Y. Gao, X. Xu, et al., Nano Res. 17 (2024) 4934–4942.
[31] Y. Gao, P. Cui, J. Liu, et al., ACS Appl. Energy Mater. 4 (2021) 4519–4529.
[32] Y. Wang, J. Chen, G. Wang, et al., Angew. Chem. Int. Ed. 57 (2018) 13120–13124.
[33] H. Fu, Z. Feng, S.S. Liu, et al., Chin. Chem. Lett. 34 (2023) 107425.
[34] Y. Jiang, Y. Qin, T. Yu, et al., Chin. Chem. Lett. 32 (2021) 1823–1826.
[35] Q. Cao, L. Wan, Z. Xu, et al., Adv. Mater. 35 (2023) 2210550.
[36] X. Suo, F. Zhang, Z. Yang, et al., Angew. Chem. Int. Ed. 60 (2021) 25688–25694.
[37] X. Tang, T. Fan, C. Wang, et al., Small 17 (2021) 2005640.
[38] W.B. Li, Y.Z. Cheng, D.H. Yang, et al., Macromol. Rapid Commun. 44 (2022) 2200778.
[39] Y. Tan, W. Chen, G. Liao, et al., Appl. Catal. B 306 (2022) 121133.
[40] W. Li, J. Wang, C. Jia, et al., J. Colloid Interface Sci. 650 (2023) 275–283.
[41] S. Yang, X. Xue, J. Zhang, et al., Chem. Eng. J. 395 (2020) 125064.
[42] E.C.H. Wen, P.H. Jacobse, J. Jiang, et al., J. Am. Chem. Soc. 145 (2023) 19338–19346.
[43] J. Li, L. Lin, D. Rui, et al., ACS Nano 11 (2017) 4641–4650.
[44] K. Gong, F. Du, Z. Xia, et al., Science 323 (2009) 760–764.
[45] K. Wang, L.M. Yang, X. Wang, et al., Angew. Chem. Int. Ed. 56 (2017) 14149–14153.
[46] P. Kuhn, M. Antonietti, A. Thomas, Angew. Chem. Int. Ed. 47 (2008) 3450–3453.
[47] Y. Dong, L. Gu, C. Wang, et al., J. Electroanal. Chem. 924 (2022) 116879.
[48] Y. Zheng, S. Chen, K.A.I. Zhang, et al., J. Colloid Interface Sci. 608 (2022) 3168–3177.
[49] N. Wang, B. Hao, H. Chen, et al., Chem. Eng. J. 413 (2021) 127954.
[50] X. Zhang, K. Zhu, C. Xie, et al., Carbon 220 (2024) 118884.
[51] R.Z. Snitkoff-Sol, O. Rimon, A.M. Bond, et al., Nat. Catal. 7 (2024) 139–147.
[52] S. Wang, J. Zhang, O. Gharbi, et al., Nat. Rev. Methods Prim. 1 (2021) 41.
[53] B. Xu, H. Zhang, X. Xia, et al., Langmuir 38 (2022) 10225–10233.
[54] Y. Xia, B. Zhu, X. Qin, et al., Chem. Eng. J. 467 (2023) 163528.
[55] L. Guo, Y Niu, S. Razzaque, et al., ACS Catal. 9 (2019) 9438–9445.